EFFECT OF FATIGUE PRE-LOADING ON HYDROGEN ASSISTED CRACKING INITIATION

V. Kharin and J. Toribio

Departamento de Ciencia de Materiales, Universidad de La Coruña (ULC)
ETSI Caminos, Campus de Elviña, 15192 La Coruña

Abstract. The effects of fatigue pre-cracking and loading rate on hydrogen assisted cracking were studied to elucidate the influence of the corresponding stress-pattern on hydrogen diffusion towards rupture sites in the crack tip zone. A finite element procedure was used to model cyclic loading using an elastoplastic large-deformation analysis combined with stress-assisted diffusion. Small scale yielding near the crack tip was addressed and characterised in terms of the stress intensity factor. In the sustained load case the test duration for reliable evaluation of the threshold was estimated. For rising loading conditions, fatigue crack closure stresses (produced by pre-cracking) affect near-tip hydrogen diffusion and consequently the whole process of hydrogen assisted fracture.

Resumen. Se han estudiado los efectos de la pre-fisuración por fatiga y la velocidad de solicitación en procesos de fisuración asistida por hidrógeno, para elucidar la influencia de las distribuciones de tensión correspondientes sobre la difusión de hidrógeno hacia los lugares de fractura en la zona del extremo de la fisura. Para modelizar la carga cíclica se ha utilizado el método de los elementos finitos, mediante análisis eleastoplástico en grandes deformaciones combinado con difusión asistida por la tensión. En el entorno del extremo de la fisura se han supuesto condiciones de plasticidad en pequeña escala caracterizadas en términos del factor de intensidad de tensiones. En el caso de carga estática se ha estimado la duración de ensayo necesaria para obtener un valor fiable del umbral. En condiciones de carga creciente, las tensiones de cierre de fisura (producidas por la pre-fisuración) afectan a la difusión de hidrógeno en el entorno del fondo de la fisura y por tanto a todo el proceso de fractura en ambiente de hidrógeno.

1. INTRODUCTION

Hydrogen has been long time recognised as a severe promoter of metals fracture [1,2] and the phenomenon of hydrogen assisted cracking (HAC) is limited by hydrogen supply to rupture sites [2]. Stress-and-strain assisted hydrogen diffusion has been substantiated as the key transport mechanism controlling the kinetics of HAC [3-5]. Modelling of hydrogen accumulation in the crack tip region has received much attention as a part of the HAC theory [5,6]. However, several items still require explanation, among them the effects of the pre-HAC crack history (i.e., fatigue pre-cracking before exposing to hydrogen) and of loading dynamics during hydrogen effect. Their interaction is of particular worth to rationalise the accelerated evaluation of materials susceptibility to HAC using dynamic rising loading, e.g., the slow strain rate testing (SSRT) technique.

A previous study of these matters [7] was based on a rough approximation of the limited data about the evolution of the elastoplastic near-tip stress field. In this paper, an advanced study is presented of hydrogen diffusion near a crack tip, accounting for fatigue pre-loading and its role on HAC initiation in SSRT. Within the framework of the diffusional theory of HAC [3-7], the problem of hydrogen diffusion affected by the crack-tip stress field is treated coupled with explicit high-resolution finite-deformation analysis of the cracked elastoplastic solid. Numerical simulation of SSRT situation is performed following the variation of the stress field from the compressive residual stresses at removed load state after fatigue cycling to the tensile stress distribution at elevated load. The implications for HAC are discussed.

2. DESCRIPTION OF THE MODEL

2.1. Basic theory

According to key ideas about HAC [5-7], elementary event of fracture facilitated by hydrogen is fixed by a critical combination of hydrogen concentration C and stress-strain state in a responsible material cell. That is, a critical value of concentration C_{cr} exists as a

function of stress and strain tensors, $\boldsymbol{\sigma}$ and $\boldsymbol{\varepsilon}$ respectively. Crack advance occur when concentration of hydrogen accumulated with time t reaches C_{cr} in a relevant location x_c near the crack tip [5-7]:

$$C(x_c,t) = C_{cr}(\boldsymbol{\sigma}(x_c,t),\boldsymbol{\varepsilon}(x_c,t)) \quad (1)$$

The left-hand part in (1) is defined by hydrogen transportation to fracture sites whereas the right-hand one depends on loading pattern. Under certain conditions, hydrogen diffusion in the metal is the rate-controlling mechanism of hydrogen supply to the fracture process zone [3-5].

Diffusion in solids depends on the density of available sites characterised by the solubility coefficient K_S and on the mobility of species represented by the diffusion coefficient D. They are sensitive to mechanical factors which may be incorporated in terms of the equivalent plastic strain $\varepsilon_{eq}{}^P$ and hydrostatic stress $\sigma = \mathrm{tr}\boldsymbol{\sigma}/3$ [3-6]. In particular, the solubility is [5,6]:

$$K_S = K_{S0}(\varepsilon_{eq}{}^P,T)\exp\left(\frac{V_H}{RT}\sigma\right) \quad (2)$$

where K_{S0} is the strain-only dependent component of solubility, T the absolute temperature, V_H the partial molar volume of hydrogen in metal and R the universal gas constant. Adopting Lagrangian description [8] of the medium and referring to current configuration of a deformed volume which at time t occupies spatial domain ${}_tV$, consideration of mass balance leads to the equation of stress-strain assisted diffusion (cf. [5-7]):

$$\frac{dC}{dt} = -\nabla\bullet\left[D\nabla C - DC\left(\frac{V_H}{RT}\nabla\sigma + \frac{\nabla K_{S0}(\varepsilon_{eq}{}^P)}{K_{S0}(\varepsilon_{eq}{}^P)}\right)\right] \quad (3)$$

For most cases, hydrogen entry may be characterised by the equilibrium value of concentration at the surface. According to (2), the diffusion boundary condition is [5-7]:

$$C|_{\text{surface}} = C_0\exp\left(\frac{V_H}{RT}\sigma|_{\text{surface}}\right) \quad (4)$$

where C_0 is the equilibrium concentration in the undeformed metal.

2.2. Finite element implementation

Large deformations of the body must be essential for near-tip diffusion since they notably change diffusion distances in the zone of interest. To solve the mechanical portion of the problem of stress-assisted diffusion at large deformations, the nonlinear finite element code MARC [9] was employed, and then complemented with a diffusion-related module.

The standard weighted residual process [10] to built up a finite-element approximation of the initial-boundary value problem (3)-(4) was performed in material (Lagrangian) coordinates taking as the reference one the instantaneous deformed configuration of the solid ${}_tV$ bounded by the surface ${}_tS$. Applying the Galerkin process for the continuum discretized into a finite elements, the same shape functions family $\{{}_tW_m;\ m = 1,2,...M\}$, M being the number of nodes in the mesh, plays the role of both trial and weighting functions.

The weak form of the weighted residual statement of the problem yields the system of equations with respect to the column of the nodal concentration values $\{C_j(t);\ j = 1,2,...M\}$ as follows:

$${}_t\mathbb{M}\left\{\frac{dC}{dt}\right\} + {}_t\mathbb{K}\{C\} = {}_t\{F\} \quad (5)$$

where the matrices ${}_t\mathbb{M}$ and ${}_t\mathbb{K}$ are defined as:

$${}_tM_{i,j} = \int_{tV} {}_tW_i\ {}_tW_j\ dV \quad (6)$$

$${}_tK_{i,j} = \int_{tV} D\left\{\nabla_t W_i\bullet\nabla_t W_j - \left[\left(\frac{V_H}{RT}\nabla\sigma(t) + \frac{dK_{S0}/d\varepsilon_{eq}{}^P}{K_{S0}}\nabla\varepsilon_{eq}{}^P(t)\right)\bullet\nabla_t W_j\right]{}_tW_i\right\}dV \quad (7)$$

and for the column in the right-hand part we have:

$${}_tF_i = -J_S\int_{tS_f} {}_tW_i\ dS \quad (8)$$

which serves to prescribe the flux of hydrogen J_S on a part ${}_tS_f$ of the body surface, if necessary. The left-hand sub-indices emphasise that the quantities refer to the instantaneous deformed configuration of the solid at time t. In numerical simulations for a loading history given in terms of the applied stress pattern $\sigma_{app}(t)$, the nodal displacements together with the stress and strain components relevant to diffusion are provided by the post-processing module of the code MARC after solution of the elastoplastic boundary-value problem. Afterwards, continuing with the diffusion simulation, mechanical fields are approximated using the same shape functions family $\{{}_tW_m\}$ as on the mechanical phase of modelling. The updated Lagrange formulation is in use as well. The time-domain Galerkin procedure [10] is employed for integration of the set of equations given in (6).

2.3. Description of the simulations

The study is confined to the small-scale yielding in obvious fracture mechanics sense. So, the tensors $\boldsymbol{\sigma}$ and $\boldsymbol{\varepsilon}$ in the crack tip zone are dominated by the stress intensity factor K. This makes the problem general in terms of $K(t) \propto \sigma_{app}(t)$ not limited to a particular body geometry and loading.

For simulations of stress-assisted diffusion, a 2D model of the double-edge-cracked panel in tension is adopted, see Fig. 1 in [11], for which mechanical aspects have already been presented in the mentioned paper. Model parameters are taken relevant to steels for which HAC has been extensively studied [2]. Namely, initial round-shape crack tip width b_0 and mechanical constants are kept the same as in the mechanical study [11] (b_0 = 5 μm, Young modulus E = 200 GPa, Poisson ratio μ = 0.3, tensile yield stress σ_Y = 600 MPa), and hydrogen-related characteristics are [3,4,7] D = 10^{-13} m²/s, V_H= 2 cm³/mol. Initial concentration of hydrogen is zero and T = 293 K. As in mechanical solution, cf. [11], the quarter-panel is considered due to the symmetry and boundary condition (8) with J_S = 0 is fixed on the primary symmetry axes.

Diffusion modelling with stationary stress field under sustained load was performed first to reveal some items related to the threshold K_{th}, and also to have a check-point concerning SSRT and pre-cracking. The reference value of K was taken K_R = 60 MPam$^{1/2}$. This is relevant to the range of HAC proceeding in materials of the type being considered [2,12,13]. In particular, it may serve as a candidate value for the HAC threshold. In the next phase, diffusion modelling with transient stress fields under SSRT conditions was considered with constant stress intensity rate $dK/dt = K^{\bullet}$ after pre-cracking by cyclic loading between zero and maximum stress intensity factor K_{max} (Fig. 1a, insert). In the modelling, K_R = 60 MPam$^{1/2}$ was used as a "candidate threshold", and K_{max} = 0.5K_R advised [14] as the proper pre-cracking limit. Several rates $K^{\bullet}$ between 0.015 and 15 MPam$^{1/2}$/min were taken to cover the range of values used in experiments [12].

The key items for HAC are the near-tip distributions of σ and $\varepsilon_{eq}{}^p$ represented in Fig. 1 as functions of the distance from the material point to the crack tip in the undeformed configuration X normalized by the current crack tip opening displacement δ_t. In the domains of low and elevated load levels, the opposite sign extrema of stress exist beyond the tip, maximum compression and tension respectively. Accordingly, the positive stress gradient associated with the latter favors hydrogen flux into metal, and the negative one with the former causes a retardation effect. The contribution of these compressive stresses is expected to be important for the near-tip diffusion, and consequently for the kinetics of HAC. Although these finite element stress-strain data [11] have similar appearance that the stress pattern approximation used in a previous diffusion simulation [7], the difference is quite significant.

3. RESULTS AND DISCUSSION

As a first approach, the finite element implementation for the problem of hydrogen diffusion was performed in a 1D approximation, i.e., on the x-axis along the crack line where element discretization, deformations and stresses were taken from the 2D mechanical solution (elastoplastic finite element computations). The study was focused on the stress effect on diffusion which is expected to be the most important in many cases, as reported elsewhere [3-6].

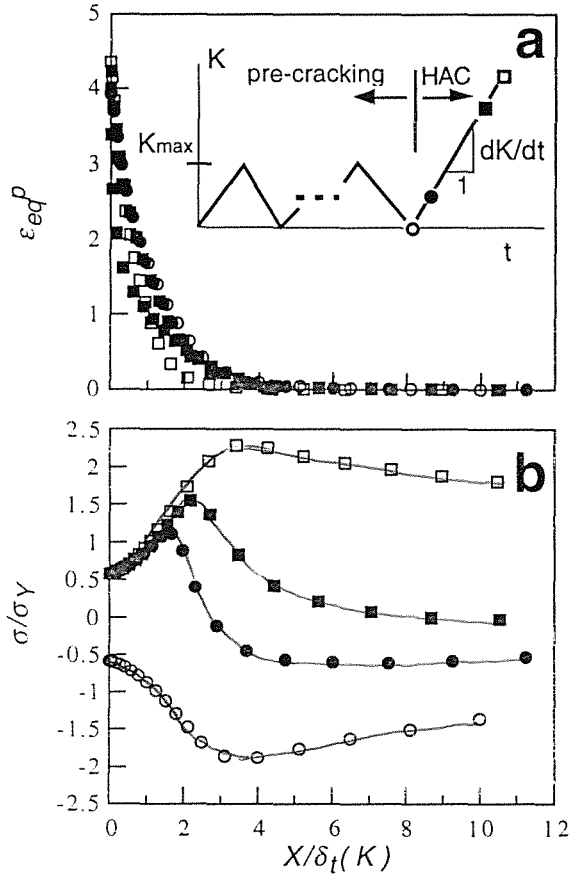

Fig. 1. Distributions of $\varepsilon_{eq}{}^p$ (a) and σ (b) along the crack line at consecutive instants of the loading history marked by corresponding symbols in the inserted scheme of the loading path.

3.1. Sustained load case

Fig. 2 displays the calculated hydrogen concentration distributions along the crack line under sustained load conditions, together with the asymptotic distribution, i.e., the approximate solution given at stationary stress $\sigma(x)$ by the long-time asymptote [7]:

$$C_{al}(x,t) = C_{eq}(x)\ \mathrm{erfc}\left(\frac{x}{2\sqrt{Dt}}\right) \qquad (9)$$

where the equilibrium distribution of concentration is

$$C_{eq}(x) = C_0 \exp\left(\frac{V_H}{RT}\sigma(x)\right) \qquad (10)$$

This latter marks the accessible upper bound for $C(x,t)$. Here x represents the diffusion distance and X is the coordinate of the material point in the deformed state.

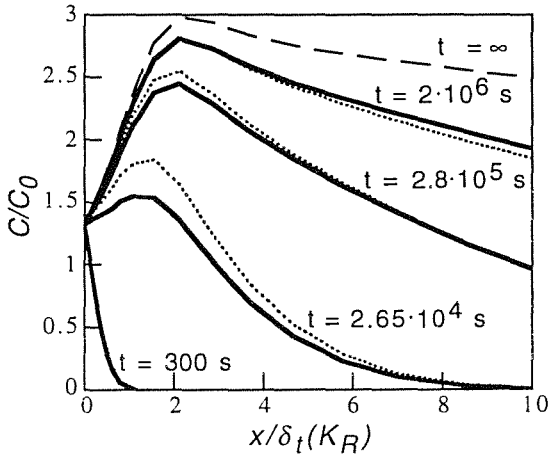

Fig. 2. Concentration distributions along the crack line under sustained load conditions: finite element solution (solid lines) and asymptotic one $C_{al}(x)$ (dotted lines). The dashed line shows the C_{eq}-profile.

Fig. 3 presents the variation of concentration in the material points of the highest interest with regard to HAC: the point $x_{m\sigma} \approx 2.3\delta_t$ where the maximum tensile stresses are attained (distributions of hydrostatic stress σ and normal stress σ_{yy} are quite similar), and the point $x_{m\varepsilon} \approx \delta_t$ which marks the zone of steeply increasing plastic strain (Fig. 1a). These are obviously considered as locations x_c of microfracture nuclei depending on the dominating fracture mechanism, stress- or strain-controlled, respectively.

These data are relevant to the HAC threshold K_{th}. Common K_{th} testing consists in trying a series of sustained K-values if crack does not start to grow within a certain waiting time t_B [15]. This time base should be properly fixed to ensure with a reasonable confidence that at K_{th} the crack will not start to grow at $t > t_B$. It is usually chosen from experience and application-related reasons [15]. Diffusion concept of HAC suggests that t_B must be about the diffusion time t_{ss} to attain at x_c the steady-state concentration with reasonable accuracy, $C(x_c,t_{ss}) \approx C_{eq}(x_c)$, the latter being able to satisfy the fracture criterion (1). Fixing, for definiteness, the tolerance level as 95% of C_{eq}, the long-time asymptote (9) renders $Dt_{ss}/x_c^2 \approx 130$. The plots in Fig. 3a confirm that the formula (9) and the numerical solution are rather close in the maximum tensile stress point $x_{m\sigma}$ within the 5% band near the equilibrium level C_{eq}. For the critical stress criterion of rupture when $x_c \approx x_{m\sigma}$ this estimate provides a basis to establish the K_{th} testing time: $t_B \geq t_{ss} \approx 130x_c^2/D$. With the chosen material parameters this test time is about 2.4×10^6 s. For strain-controlled fracture, at $x_c \approx x_{m\varepsilon}$ numerical solution evolves slower than the asymptote (9), and the estimates for t_{ss} and t_B must be stiffened to about $t_B \approx 440x_c^2/D$. However, due to shorter diffusion path in this case, the time estimate is 20-times shorter, $t_B \approx 1.2 \cdot 10^5$ s.

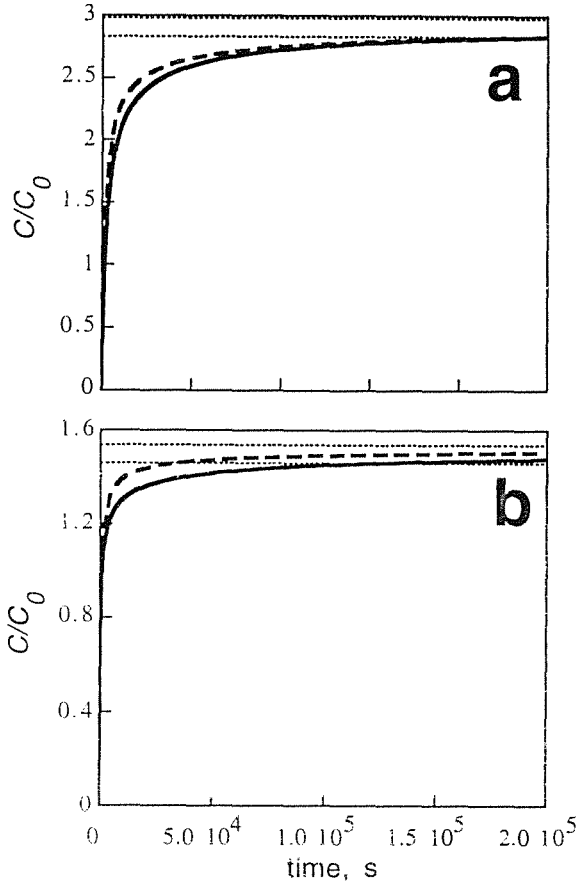

Fig. 3. Concentration evolutions according to the finite element solution (solid curves) and asymptotic one (9) (dashed curves) at sustained load: (a) in the points of maximum tensile stress $x_{m\sigma}$; (b) in the high plastic strains region at $x_{m\varepsilon}$. Horizontal lines mark the 5%-tolerance band near the corresponding equilibrium concentration levels $C_{eq}(x)$.

3.2. Rising load case

This series of the diffusion simulations reveals the importance of crack closure stresses in HAC when the SSRT technique is used in experimental evaluation of environment-sensitive cracking [15]. In this case a single dynamic test is performed with rising load to pass the whole stress intensity range up to detecting a crack growth initiation at some K_R which could be the desired K_{th}. To render the adequate threshold, the concentration at the time $t_R = K_R/K^\bullet$ must reach $C_{eq}(K_R,x_c)$ with a reasonable accuracy as in a sustained load test. These tests are performed starting from zero load after fatigue pre-cracking in inert environment. Hydrogenation proceeds affected by the residual stresses caused by pre-cracking.

Calculated concentration distributions for $K^\bullet = 1.5$ MPam$^{1/2}$/min are shown in Fig. 4 together with the corresponding hydrostatic stress profiles.

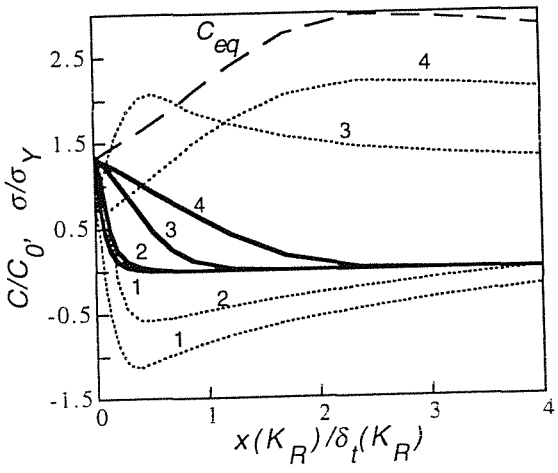

Fig. 4. Finite element solutions for concentration (solid lines) and hydrostatic stress (dotted lines) beyond the crack tip at different times under dynamic load at $K^\bullet$ = 1.5 MPam$^{1/2}$/min. The dashed line shows the equilibrium concentration distribution. Curves 1-4 refer respectively to times of 180, 300, 1000 and t_R=2400 s.

Concentration evolutions in the points of maximum tensile stresses and large plastic strains, $x_{m\sigma}(K_R)$ and $x_{m\varepsilon}(K_R)$ respectively, are plotted in Fig. 5. For comparison, the $\sigma(t)$-patterns are also presented, as well as the variations of $C_{al}(\sigma)$ corresponding to the instantaneous stress values $\sigma(x_{m\varepsilon,m\sigma},t)$ according to formula (10). For slower loading and rather short diffusion depth $x_{m\varepsilon}$ the analytical form goes closely to the finite element solution. Thus, in the very near-tip domain, diffusion under dynamic load nearly attains the equilibrium saturation for the instantaneous stress. In the relatively remote point $x_{m\sigma}$ the delay of hydrogenation is notable even at the slowest loading.

These data can be considered as a SSRT simulation to determine K_{th}, and the reference K_R may be assumed as the apparent HAC threshold already measured using the sustained load method modelled in the previous section. The threshold status is reached by approaching the equilibrium concentration in a material point x_c. If the critical concentration (1) is stress- controlled, rupture is associated with the maximum tensile stress and occurs at $x_c = x_{m\sigma}(K_R)$. To provide sufficient concentration there at the moment of approaching the critical stress intensity factor, (K_R as supposed) the loading must be much slower than tried in our simulations, and the slower the better to reproduce the result of the sustained load test. The reasonable loading rate here may be estimated so that the time $t_R = K_R/K^\bullet$ necessary to attain this candidate threshold K_R were close to t_{ss} for the stationary load situation.

However, if critical concentration (1) is strain-controlled, the problem is more complicated. At slow loading rate, concentration evolution in the large-strain zone $x \lesssim x_{m\varepsilon}$ chases after the non-monotonous $\sigma(t)$-history which depends on the residual compressive stresses from pre-cracking. Correspondingly, during not too fast loading the concentration in the intensively strained region may temporarily exceed the level attainable there in sustained load test. This was observed in simulations with $K^\bullet$ up to 0.15 MPam$^{1/2}$/min, but disappeared at 1.5 MPam$^{1/2}$/min. This means that the same fracture criterion (1) may be satisfied there earlier than in sustained load case, at times of the order of 10^4 s. This is a very important point: because of the described temporal (and early) concentration peaks, HAC may start at K below the apparent threshold from the sustained load test, depending on the particular role of stress and strain factors in the critical concentration (1).

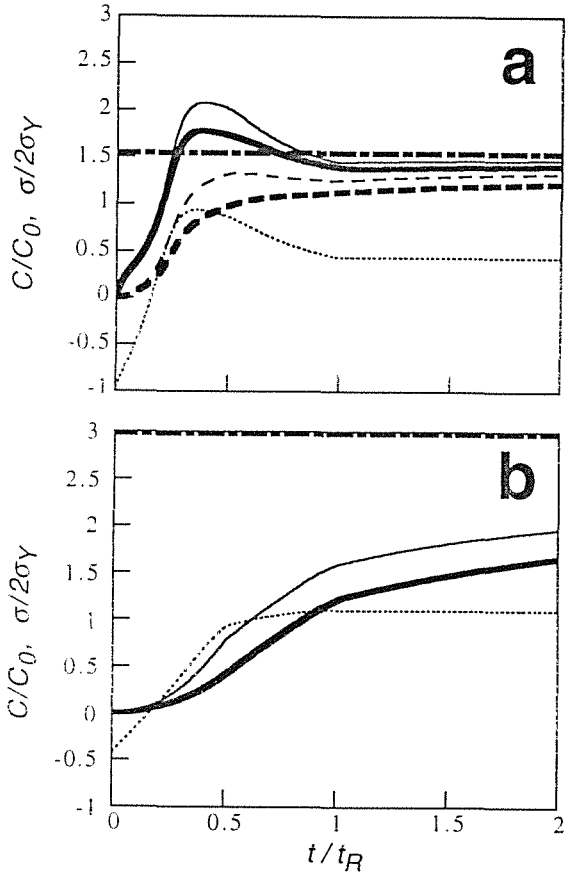

Fig. 5. Concentration evolutions under dynamic loading according to the finite element solution (bold lines) and the equilibrium one (10) (thin lines): (a) in the supposed border of the large plastic strain region at $X_{m\varepsilon}$; (b) in the points $X_{m\sigma}$ of maximal tensile stress. Solid lines correspond to $K^\bullet$ = 0.15 MPam$^{1/2}$/min and dashed lines to $K^\bullet$ = 1.5 MPam$^{1/2}$/min (in plot (b) the concentrations corresponding to this latter case are negligible). Thin dotted lines show hydrostatic stress, and bold dashed-dotted lines mark the steady-state levels of C_{eq} at $K = K_R$ in respective locations.

4. CONCLUSIONS

Stress-assisted hydrogen diffusion near a stationary crack tip was studied with relevance to hydrogen assisted cracking (HAC) using large-deformation finite-

element analysis. Hydrogen diffusion was modelled for sustained and rising loading preceded by fatigue pre-cracking with reference to corresponding experimental techniques of HAC threshold evaluation.

In the sustained load case, the adequate testing time to approach the threshold (the steady-state concentration). depends on the location of the critical material cell near the crack tip which is associated with the dominating factor of local rupture (plastic strain or tensile stress).

Under conditions of dynamic rising loading after fatigue load removal, the effects of crack closure stresses from the pre-HAC loading history may affect hydrogen diffusion towards rupture sites. In the range of the slow loading rates, rupture may occur earlier than in the sustained load case at otherwise similar circumstances if critical hydrogen concentration (fracture mechanism) is strain-controlled, due to the temporal hydrogen over-saturation peaks which arise owing to the peculiarities of the stress evolution patterns at dynamic loading.

The described premature fractures in the rising load case can occur at K-levels even lower than in the sustained load case. This means that the latter can produce excessively optimistic over-estimations of the HAC resistance characteristics of materials in comparison with SSRT. However, all that depends essentially on the dominance of the potentially responsible factors (stress and plastic strain) in a specific material under particular conditions.

Further modelling of the near-tip stress-strain assisted hydrogen transport in metals involving consideration of particular stress-and-strain driven rupture mechanisms (and corresponding criteria) will be helpful to explain various features and manifestations of the phenomenon of hydrogen assisted fracture.

Acknowledgements
This work was funded by the Spanish CICYT (Grant MAT97-0442) and Xunta de Galicia (Grants XUGA 11801B95 and XUGA 11802B97). One of the authors (VKh) is indebted to DGICYT (Grants SAB95-0122 and SAB95-0122P) and Xunta de Galicia for supporting his stays as sabbatic professor and visiting scientist at the University of La Coruña.

REFERENCES

1. Hirth, J.P. and Johnson, H.H., Hydrogen problems in energy related technology, *Corrosion* 1976, **32**, 3-15.
2. Nelson, H.G., Hydrogen embrittlement, in: *Treatise on Materials Science and Technology.* Vol. 25, Academic Press, New York, 1983, pp. 275-359.
3. Van Leeuwen, H.-P., The kinetics of hydrogen embrittlement: a quantitative diffusion model. *Engng. Fract. Mech.* 1974, **6**, 141-161.
4. Gerberich, W.W., Chen, Y.T. and John, C.St., A short-time diffusion correlation for hydrogen-induced crack growth kinetics. *Met. Trans. (A)* 1975, **6**, 1485-1498.
5. Toribio, J. and Kharin, V., K-dominance condition in hydrogen assisted cracking: t.he role of the far field. *Fatigue Fract. Engng. Mater. Struct.* 1997, **20**, 729-745.
6. Toribio, J. and Kharin, V., Interaction between hydrogen diffusion and crack growth in hydrogen assisted cracking, in: *Advances in Fracture Research* (ICF9, Sydney, 1997), Amsterdam, Pergamon Press, 1997, pp. 343-350.
7. Kharin, V. and Toribio, J., Modelling hydrogen diffusion in metals near a blunting crack tip, *Anales Mec. Fract.* 1997, **14**, 93-98.
8. Malvern, L.E., *Introduction to the Mechanics of a Continuous Medium*, Prentice Hall, Englewood Cliffs, 1969.
9. *MARC User Information*, Palo Alto, 1994.
10. Zienkiewicz, O.C. and Morgan, K., *Finite Elements and Approximation*, John Wiley and Sons, New York, 1983.
11. Kharin, V. and Toribio, J., Alternating stress-strain fields near the crack tip under cyclic loading. *Anales Mec. Fract.* 1998, **15**.
12. Mayville, R.A., Warren, T.J. and Hilton P.D., Determination of the loading rate needed to obtain environmentally assisted cracking in rising load tests. *J. Test. Eval.* 1989, **17**, 203-211.
13. Loginow, A.W. and Phelps, E.H., Steels for seamless hydrogen pressure vessels. *Corrosion* 1975, **31**, 404-412.
14. Judy, R.W., Jr., King, W.E, Jr., Hauser II, J.A. and Crooker, T.W, Influence of experimental variables on the measurement of stress corrosion cracking properties of high-strength steels, in: *Environmentally Assisted Cracking: Science and Engineering, STP 1049*, American Society for Testing and Materials, 1990, pp. 410-422.
15. Turnbull, A., Test methods for environment assisted cracking. *Brit. Corros. J.* 1992, **27**, 271-289.